Oxygen content and superconductivity in $Y_{0.8}Ca_{0.2}Ba_2Cu_3O_y$ ($y=6.03-6.89$)

J. Hejtmánek, Z. Jirák, and K. Knížek
Institute of Physics, 162 00 Prague 6, Czech Republic

M. Dlouhá and S. Vratislav
Faculty of Nuclear Physics and Physical Engineering, 180 00 Prague 8, Czech Republic

(Received 23 April 1996)

The $Y_{0.8}Ca_{0.2}Ba_2Cu_3O_y$ samples with a large range of oxygen content, equilibrated at 460 °C, have been prepared under reducing or oxidizing conditions from a well sintered master batch of nearly 100% compactness. The investigation by the x-ray and neutron diffraction methods and by the resistivity, thermoelectric power, Hall effect, and magnetic susceptibility measurements have shown three distinct superconducting plateaus depending on the decreasing oxygen content. The first two plateaus correspond to T_c of about 80 K ($6.89 \geqslant y \geqslant 6.75$) and 50 K ($6.75 \geqslant y \geqslant 6.50$) and are associated with the ortho I and II structures which are characterized with infinite Cu-O chains. The third plateau corresponds to a macroscopically tetragonal phase with $T_c=25$ K ($6.50 \geqslant y \geqslant 6.40$) and is possibly associated with formation of the Cu-O-Cu dimers. All three superconducting phases exhibit sharp magnetic transitions with nearly complete diamagnetism at low temperatures and a metalliclike electric conductivity in the normal state. The hole concentration as deduced from the calculated bond valence sums (BVS) smoothly decreases with decreasing y without apparent steps. For $6.89 \geqslant y \geqslant 6.36$ the BVS values are in good agreement with the number of itinerant carriers deduced from the Hall data. In the nonsuperconducting phase with $y=6.33$, the sudden decrease of the Hall number and simultaneous temperature activation of the Hall constant and resistivity indicate a localization of carriers below 300 K. Nevertheless, the Hall mobility remains compositionally independent for all samples with $6.89 \geqslant y \geqslant 6.33$. [S0163-1829(96)07846-0]

I. INTRODUCTION

Among possible cationic substitutions in the $YBa_2Cu_3O_y$ superconductor, the partial replacement of Y^{3+} by Ca^{2+} has been found to be especially interesting. The heterovalent substitution changes the carrier concentration and may influence the charge transfer from the Cu-O chains to the conducting CuO_2 layers. Early studies have shown that such replacement was limited to about 25% of yttrium and the critical temperature for the superconductivity in the orthorhombic samples ($y \sim 7$) was lowered from 93 K for the calcium free compound to about 78 K for 20% of calcium.[1,2] For the latter compound, the superconductivity was detected also for highly reduced tetragonal samples ($y=6.0-6.2$). This surprising behavior was reported first for nearly 100% dense ceramics cooled from 950 °C by switching off the furnace.[2] The occurrence of superconductivity was ascribed to a surface oxidation of otherwise oxygen-deficient crystal grains. However, the superconductivity at temperatures as high as 44 K was subsequently observed on assumedly homogeneous samples with 20% of Ca, prepared under reducing conditions and quickly quenched.[3]

A systematic study of the parent compound $YBa_2Cu_3O_y$ was performed namely by Jorgensen *et al.*[4] and by Cava *et al.*[5] on samples prepared by quenching from controlled oxygen partial pressures at 520 °C and on a series of samples gettered in sealed ampoules at 440 °C by zirconium, respectively. In both studies, no superconductivity was detected in tetragonal phase below $y=6.4$. In order to investigate complexly the hole doping and the interlayer charge transfer also in the calcium substituted systems, we have undertaken simultaneous structural (x-ray and neutron diffraction), transport (electrical resistivity, thermoelectric power, Hall effect), and magnetic (ac susceptibility) studies on the $Y_{0.8}Ca_{0.2}Ba_2Cu_3O_y$ ceramics within the whole accessible range of y.

II. EXPERIMENTS

The master batch of about 150 g of $Y_{0.8}Ca_{0.2}Ba_2Cu_3O_y$ has been prepared from homogenized mixture of chemically analyzed Y_2O_3, $CaCO_3$, $BaCO_3$, and CuO. The mixture was calcinated several times at progressively increasing temperatures 850–930 °C with intermediate homogenization and weighting in order to improve the spacial homogeneity of reagents and to control the decomposition of carbonates. The calcinate was pressed into pellets of 20 mm in diameter and width of 3 mm and sintered for 48 h at 940 °C. The temperature was then decreased to 600 °C and kept for 2 h. That was followed by slow cooling (0.5 °C min) to 460 °C and dwelling for 100 h at this temperature. The pellets were then cooled rather quickly by switching off the furnace. The whole sintering procedure was undertaken in oxygen atmosphere.

Such prepared $Y_{0.8}Ca_{0.2}Ba_2Cu_3O_y$ ceramics exhibited 98% of the theoretical density and sharp superconducting transition at 81 K, resulting in an ideal diamagnetic ac signal at low temperatures. The oxygen content of this starting material was estimated, as described below, from the unit cell dimensions ($a=3.8351$ Å, $b=3.8721$ Å, $c=11.679$ Å) to $y=6.82$ and the homogeneity of the calcium distribution within crystal grains was checked by the electron mi-

croanalysis. A quantitative analysis of the x-ray diffraction pattern showed that calcium substituted yttrium sites in the structure in the expected amount of 20(1)%.

By heating at 460 °C in an oxygen pressure of 12 atm, the oxygen content in the material was further slightly increased ($y=6.89$) without any significant change of the superconducting temperature. Annealing of the starting material under argon flow for 24 h at 600 °C and subsequently at 460 °C with 100 h duration led to the product with $T_c \sim 40$ K and 91% of complete diamagnetism at low temperatures. Lattice parameters of the tetragonal structure $a=3.8582$ Å and $c=11.750$ Å enabled us to estimate the oxygen content to $y=6.34$. Subsequent equilibrating of the sample at 460 °C in evacuated ampoule led to a disappearance of any traces of superconductivity. Since the lattice parameters of such treated sample were retained, the superconductivity of argon annealed sample was ascribed rather to a surface oxidation of crystalline grains during the cooling from 460 °C in technical argon gas (oxygen partial pressure 10^{-4}). Finally, the oxygen and argon treated materials were simultaneously annealed in the nitrogen flow (oxygen partial pressure 10^{-4}) at 460 °C for 100 h. This procedure led to samples with $y=6.62$ and $y=6.51$, respectively.

Oxygen content of $Y_{0.8}Ca_{0.2}Ba_2Cu_3O_y$ samples, obtained in the oxygen, nitrogen, or argon flows ($y=6.82$, 6.62, 6.51, and 6.34), was then systematically changed by long-time annealing in sealed quartz ampoules or in evacuated ampoules with variable amount of Zr granules. Since no gettering effect of metallic Zr was observed below 550 °C, the ampoules were generally heated to 600 °C with duration for 50 h and subsequently cooled to 460 °C and annealed for 150 h.

The Cu K_α x-ray diffraction patterns were recorded for all samples immediately after their preparation. In the case of reduced samples, the structure was checked after more than one month in order to monitor an eventual oxygen uptake. No change was observed for oxygen content down to $y \sim 6.3$ even if the material was kept pulverized into fine particles at room temperature. On the other hand, the maximum reduced pellet with $y=6.03$ showed a bulk gain of oxygen (to $y=6.13$) after two months. Such behavior can be related to possible deterioration of sintered ceramics when the reduction achieved the absolute limit.

For five selected samples ($y=6.13$–6.89), a complete structural determination was achieved by neutron diffraction. The experiments were performed at room temperature on the diffractometer KSN-2 in Řež near Prague using the neutron wavelength of 1.365 Å and the arrangement of the best resolution ($\Delta d/d=0.007$ in the minimum). The analysis of observed x-ray and neutron diffraction patterns was performed by the program FULLPROF.

A classic four probe dc method was used for the resistivity measurements in the range of 4.2–300 K. Small platelets were cut from the pellets and four electrical contacts of about 0.01 mm^2 on the circumference of the sample were made using silver paint and fired at 400 °C under flowing oxygen or in vacuum, depending on the actual oxygen content in the samples. Absolute values of the electrical resistivity were evaluated using the Van der Pauw method.

A dynamic two point method was employed for the measurement of the thermoelectric power. The platelets were attached to two small copper blocks and a variable temperature gradient up to 1 K was developed between the copper blocks. The gradient was created by two miniheaters and monitored using Pt resistors. The assembly was placed in a closed cycle He cryostat and the measurements were carried out while slowly increasing the temperature from 15 to 300 K. The thermoelectric voltage vs temperature gradient was monitored and used for the calculation of the thermopower coefficient.

ac magnetic susceptibility measurements were carried out in the temperature range 4.2–300 K using an inductance method. The frequency of the ac field was set to 160 Hz and its amplitude to 40 $A\,m^{-1}$. Both the in-phase and out-of-phase signals from the secondary coils were measured approximately every 0.2 K with a help of the lock-in nanovoltmeter and absolute values of the real and imaginary parts of the magnetic susceptibility were evaluated using the reference specimen. A rectangular form of the samples was approximated by a general ellipsoid and a correction on the demagnetizing field was made according to Ref. 6.

Hall effect measurements were carried out for thin rectangular plate samples. The electrical contacts for samples with $y>6.5$ were made similarly as for the resistivity measurements and a short-time annealing in air at 300 °C was used to decrease the resistance of contacts below 100 Ω. Those for low oxygenated samples were made by a spark bonding of 50 μm Cu wire. Low contact resistance (less than 10 Ω) was achieved by a subsequent joule heating of silver paint applied to the contact area. The Hall voltage V_H was measured using the lock-in technique. The current density, applied within the plate, did not exceed 1 $A\,cm^{-2}$ and the frequency of the ac signal was set to 16 Hz. The Hall constant R_H was then calculated from the slope of the V_H vs B dependence when the magnetic field B was swept between -2 and 2 T at fixed temperature.

III. RESULTS

A complete list of studied $Y_{0.8}Ca_{0.2}Ba_2Cu_3O_y$ specimens is given in Table I. The sample numbers follow the decreasing oxygen content and evolution of the structural and transport properties. Preparation conditions and the initial composition are mentioned for each sample. The samples are characterized with the unit cell dimensions and volume, the room temperature values of the thermopower coefficient S_{290}, and the superconducting critical temperatures T_c. Except for three samples mentioned in Table I, the T_c values inferred from the sharp drop of the thermoelectric power towards zero (see Fig. 1) match with the onset of the zero electrical resistivity as well as the diamagnetism in the ac susceptibility measurements. This coincidence is evidenced for selected samples in Figs. 1–3.

The oxygen content in $Y_{0.8}Ca_{0.2}Ba_2Cu_3O_y$ was determined for five samples by the neutron diffraction, for other ones it was estimated under the assumption of a linear relationship between the y value and the c lattice parameter which is shown in Fig. 4. This correlation follows from the mentioned neutron data as well as from the value of the c parameter of 11.800 Å which was observed for a series of maximum reduced samples and identified with stoichiometry $y \sim 6.0$. Indeed, all attempts to further decrease the oxygen

TABLE I. Characterization of the $Y_{0.8}Ca_{0.2}Ba_2Cu_3O_y$ samples.

Class	No.	a (Å)	b (Å)	c (Å)	V (Å^3)	S_{290} (μV K^{-1})	T_c (K)[c]	y	Annealing (initial composition)	
A	1	3.8341(5)	3.8735(5)	11.668(1)	173.34	2	80	6.89(3)[b]	12 atm O2	(6.82)
	2	3.8351(7)	3.8721(8)	11.679(2)	173.43	2	81	6.82	O2 flow	(as prepared)
	3[a]	3.8354(5)	3.8742(5)	11.683(1)	173.60	8	74	6.79	Evacuated ampoule	(6.82)
B	4	3.8496(5)	3.8647(6)	11.693(2)	173.93	20	52	6.72	Zr gettered	(6.79)
	5	3.8492(8)	3.8645(9)	11.708(3)	174.16	20	51	6.62	N2 flow	(6.82)
	6	3.8502(7)	3.8650(8)	11.719(2)	174.38	19	52	6.52(2)[b]	Evacuated ampoule	(6.62)
	7[a]	3.8576(8)	3.8617(8)	11.712(2)	174.29	27	30	6.59	Zr gettered	(6.79)
C	8	3.8544(9)	3.8605(10)	11.728(2)	174.51	37	25	6.51	N2 flow	(6.34)
	9	3.8586(4)		11.729(1)	174.63	41	27	6.50(2)[b]	Evacuated ampoule	(6.51)
	10	3.8592(4)		11.726(2)	174.64	40	22	6.48	Oxidated in amp.	(6.34)
	11	3.8582(5)		11.739(2)	174.75	39	25	6.41	Oxidated in amp.	(6.34)
D	12	3.8581(5)		11.747(2)	174.85	60		6.36	Zr gettered	(6.41)
	13	3.8593(5)		11.743(2)	174.91	65		6.38	Zr gettered	(6.52)
	14[a]	3.8582(6)		11.750(2)	174.91	40	25	6.34	Ar flow	(6.82)
	15	3.8580(6)		11.754(2)	174.95	66		6.33(2)[b]	Zr gettered	(6.34)
	16	3.8590(5)		11.766(2)	175.22	90		6.23	Oxidated in amp.	(6.03)
	17	3.8585(3)		11.776(1)	175.32	100		6.13(2)[b]	Aged 2 months	(6.03)
	18	3.8582(5)		11.795(2)	175.58	145		6.03	Zr gettered	(6.33)

[a]Nonhomogeneous samples: Two-step resistivity transition at 76 and 50 K for No. 3; Resistivity transition 50–30 K, diamagnetic at 47 K for No. 7; Resistivity and diamagnetic transition at 40 K for No. 14.
[b]Based on the neutron diffraction data.
[c]Inferred from the thermopower data.

content always led to an occurrence of Cu_2O on the sample surface.

The y values in Table I represent, in our opinion, the most reliable estimates of the oxygen content. Alternative determination of the oxygen stoichiometry was attempted by a cerimetric titration using a trapping Fe^{2+}/Fe^{3+} system in hydrobromic solution. For samples with oxygen content determined by the neutron diffraction to $y=6.89$, 6.52, 6.50, and 6.33 (experimental uncertainty of $\Delta y\sim 0.02$), the cerimetry gave values 6.91, 6.58, 6.45, and 6.36, respectively. Small differences up to $\Delta y=0.06$ may reflect the poorer accuracy of the chemical method. Larger deviation from the neutron data was found for sample with $y=6.13$. This was ascribed to a change of the oxygen content in this particular sample with time, which was already mentioned in Sec. II. For other investigated samples with oxygen content estimated from the c vs y relationship to $y=6.82$, 6.72, 6.62, 6.41, 6.36, and 6.23, the cerimetry resulted in values 6.77, 6.64, 6.55, 6.40, 6.34, and 6.23, respectively.

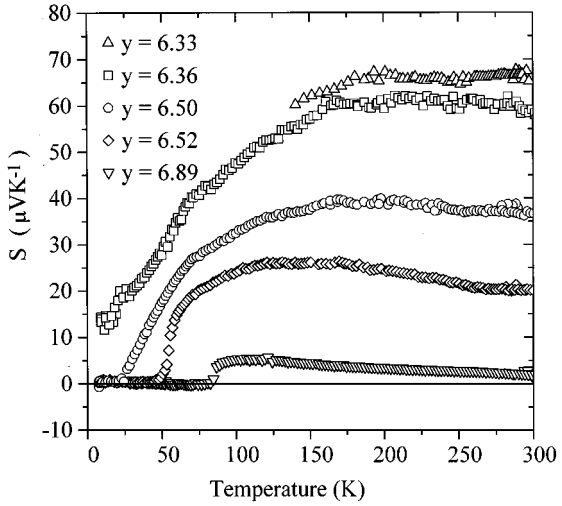

FIG. 1. The temperature dependence of thermopower in $Y_{0.8}Ca_{0.2}Ba_2Cu_3O_y$.

As illustrated in Fig. 4, one can distinguish four thermodynamically stable regions or phases in the $Y_{0.8}Ca_{0.2}Ba_2Cu_3O_y$ system. Within these regions, the oxygen content can be varied in certain limits but the orthorhombic distortion, the thermopower coefficient S_{290} and the critical temperature T_c remain essentially unchanged. In the first, oxygen rich region A ($6.89\geqslant y\geqslant 6.75$), the orthorhombic distortion is set close to 0.039 Å, the superconducting temperature reaches 80 K, and the room temperature thermopower, in agreement with the high T_c, is near zero. The second region B spanning from $y\sim 6.75$ to $y\sim 6.50$ is also orthorhombic with significantly lower distortion $(b-a)\sim 0.015$ Å, the thermopower coefficient amounts to $S_{290}\sim 20$ μV K^{-1} and T_c is lowered to about 50 K. The third region C from $y\sim 6.50$ to $y=6.40$ is characterized by tetragonal or pseudotetragonal [$b-a=0.000(2)$ Å] symmetry. The thermopower coefficient equals $S_{290}\sim 40$ μV K^{-1} and $T_c\sim 25$ K. All three superconducting regions exhibit a metallic conductivity in the normal state (Fig. 2). A temperature dependent Hall constant R_H for sample $y=6.89$, which increases from about 10^{-9} m^3 C^{-1} at 290 K to 3.10^{-9} m^3 C^{-1} at 90 K, is followed up with rather temperature independent Hall constant for samples $y=6.52$ ($R_H=4\times 10^{-9}$ m^3 C^{-1}) and $y=6.50$ ($R_H=7\times 10^{-9}$ m^3 C^{-1})—see Fig. 5.

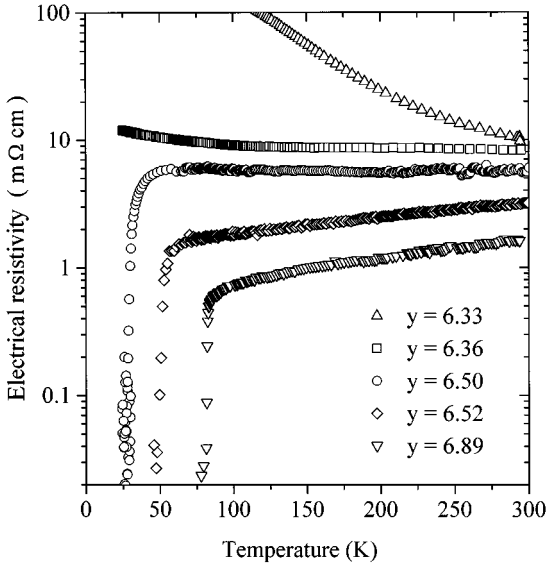

FIG. 2. The temperature dependence of resistivity in $Y_{0.8}Ca_{0.2}Ba_2Cu_3O_y$.

The last, oxygen poor region D ($6.40 \geqslant y \geqslant 6.03$) is nonsuperconducting. The thermopower coefficient smoothly increases with decreasing y from $S_{290}=60\ \mu V\,K^{-1}$ to $145\ \mu V\,K^{-1}$. This region is characterized by a semiconducting turn-up of the resistivity which shifts with decreasing y quite quickly from low temperatures up to the room temperature—see Fig. 2 for samples $y=6.36$ and 6.33. Simultaneously with the shift of the temperature activation of electrical resistivity to room temperature, a large and strongly temperature dependent constant R_H is observed (see Fig. 5).

With respect to the formation of four distinct regions $A-D$ there are three samples in Table I which should be considered as intermediate even after long-time annealing in sealed ampoules. Sample No. 3 with thermopower $S_{290}=8\ \mu V\,K^{-1}$ showed a two-step transition with $T_{c1}=76$ K and

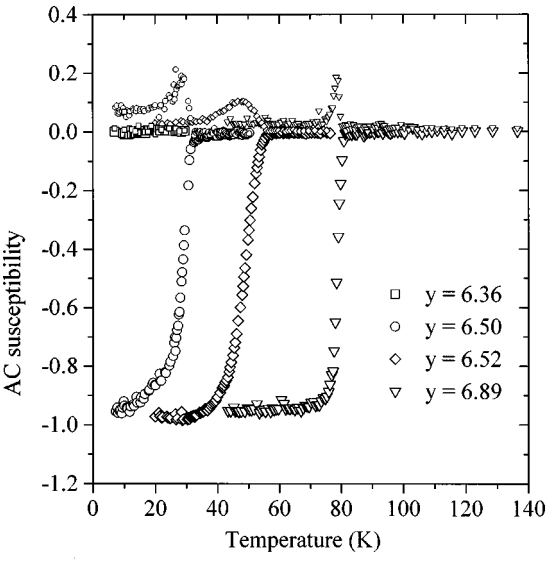

FIG. 3. The real and imaginary parts of the ac susceptibility in $Y_{0.8}Ca_{0.2}Ba_2Cu_3O_y$.

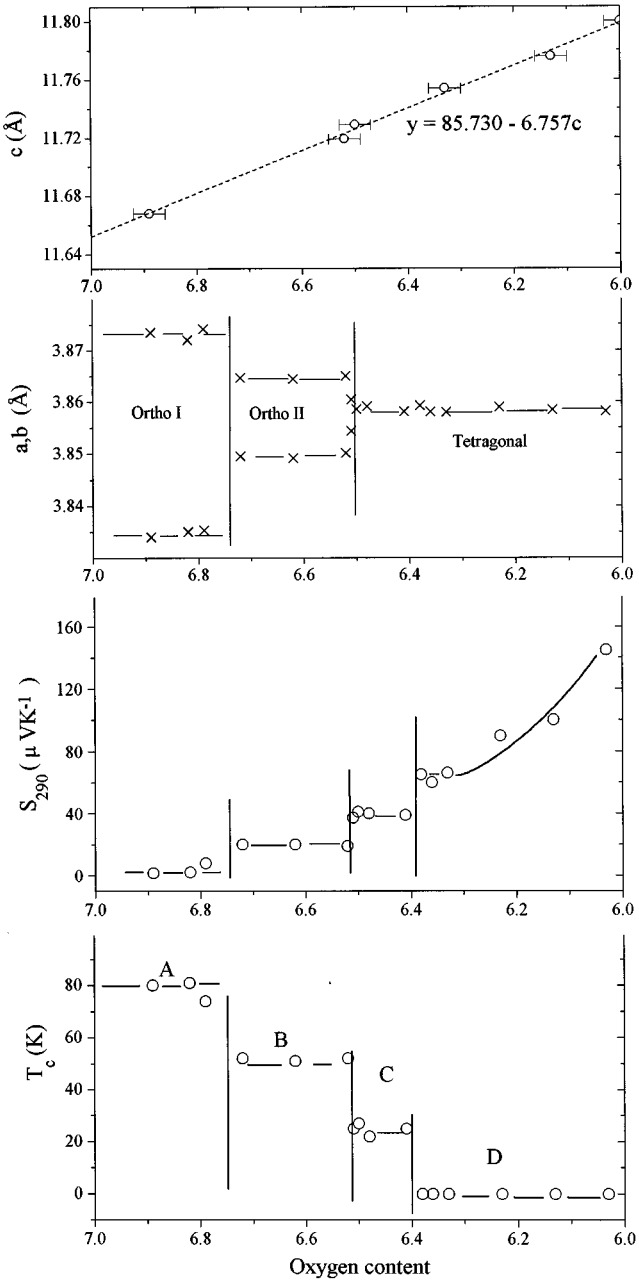

FIG. 4. The superconducting temperatures T_c, thermopower coefficients $S290$, and the room-temperature lattice parameters of $Y_{0.8}Ca_{0.2}Ba_2Cu_3O_y$ in dependence on oxygen content y.

$T_{c2}=50$ K in the resistivity measurement and represents therefore a mixture of the A and B types. Sample No. 7 with $S_{290}=27\ \mu V\,K^{-1}$ exhibited an extremely broad resistivity transition between 50 and 30 K and can be considered as a mixture of the B and C types. The same thing most probably occurs also for sample No. 8 which exhibits very small orthorhombicity. Otherwise, its transport properties are characteristic for tetragonal samples of the C type.

The most ideal representatives of the superconducting types A, B, and C and two samples belonging to the oxygen rich and poor side of the nonsuperconducting range D have been investigated by the powder neutron diffraction. The results of the structural refinement within the space groups

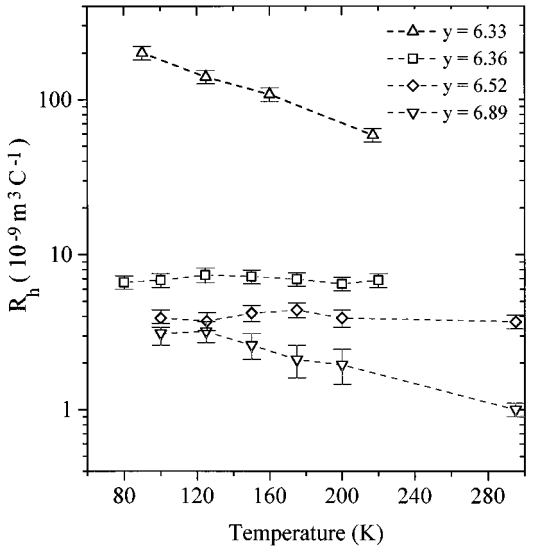

FIG. 5. The Hall number R_H for selected samples of $Y_{0.8}Ca_{0.2}Ba_2Cu_3O_y$.

Pmmm and *P*4/*mmm* for the orthorhombic and tetragonal phases, respectively, are summarized in Table II.

IV. DISCUSSION

The present study confirms a previous observation in Ref. 2 that the calcium substitution in $Y_{0.8}Ca_{0.2}Ba_2Cu_3O_y$ promotes the sintering process so that the material exhibits nearly 100% of theoretical density. This has a positive effect on the long-time room temperature stability of the ceramics against oxygen gain or loss. High compactness may explain also the necessity of annealing temperature as high as 460 °C and times of about 150 h for redistribution of variable oxygen throughout the crystal grains. Otherwise, in a ceramics with pores and voids the oxygen exchange might persist to considerably lower temperatures. We note that, e.g., Jorgensen *et al.* achieved an equilibrium after annealing for 300 h of a mixture of $YBa_2Cu_3O_{6.92}$ and $YBa_2Cu_3O_{6.09}$ in sealed ampoule at 350 °C.[4]

One of the important findings of the neutron diffraction performed on the $Y_{0.8}Ca_{0.2}Ba_2Cu_3O_y$ system is the linear increase of the *c* lattice parameter with decreasing oxygen content *y* as shown in Fig. 4. Similar behavior was reported for $YBa_2Cu_3O_y$ by Jorgensen *et al.*,[4] except for a small irregularity near the orthorhombic-tetragonal transition which in fact we cannot rule out in the present system. The comparison of our results with Ref. 4 suggests that in the whole region of the oxygen content the *c* parameter is shortened due to the Ca substitution roughly to about 0.035 Å. Somewhat different data on $YBa_2Cu_3O_y$ were published by Cava *et al.*[5] They refer, however, to the helium temperature so that the comparison is not straightforward.

The structure of the $YBa_2Cu_3O_y$ type consists of a sequence of atomic layers which play different roles in the carrier doping and charge transfer. Two copper cations per formula unit occupy sites Cu2 in the CuO_2 planes, considered as the main conducting part of the superconductor, and one copper cation occupies the Cu1 site in the CuO_δ plane of variable oxygen content ($\delta=7-y$). In the orthorhombic region ($y=7-6.4$ for $YBa_2Cu_3O_y$) the oxygen atoms in the CuO_δ plane are located preferentially in sites [0 1/2 0] and form characteristic Cu-O chains along the *b* direction. The occupation of alternative sites [1/2 0 0] is generally very small.[4] For lower *y* values the structure is macroscopically tetragonal because the oxygen atoms are distributed equally over the [0 1/2 0] and [1/2 0 0] sites or, for $y=6$ are eventually absent.

It should be noted that in addition to the special case $y=7$ (so called ortho I phase), several ordered variants with partial oxygen population were detected in single crystal studies of $YBa_2Cu_3O_y$. There are reports on pseudotetragonal phases for $y\sim6.35$ in which the Cu-O-Cu dimers are formed in the CuO_δ plane.[7–9] Further reported structures correspond to the orthorhombic phase with ideal composition $y=6.5$ (ortho II phase)[7,10,11] and $y=6.667$ (ortho III phase)[12] in which infinite Cu-O chains alternate with the Cu rows. The ortho II phase is observed in a rather broad region of *y* which actually overlaps with the ideal composition for ortho III. These superstructures are generally not visible in powder diffraction since the coherent regions are extremely small.

The present structural data on $Y_{0.8}Ca_{0.2}Ba_2Cu_3O_y$ report, therefore, only indirectly on the oxygen ordering in the CuO_δ plane. Since a trial refinement of diffraction data for $y=6.89$ excluded a significant occupation of the alternative oxygen [1/2 0 0] sites, we ascribe the first superconducting region $y=6.89-6.75$ to the ortho I structure with infinite, slightly oxygen vacant Cu-O chains. Nevertheless, the observed orthorhombic deformation $b-a=0.039$ Å is markedly smaller than the corresponding value of 0.065 Å observed for the calcium free $YBa_2Cu_3O_y$. We relate such small orthorhombicity to an increased oxidation state of copper in chains due to calcium substitution. This assumption is confirmed by the analysis of bond valence sums which is described below.

The second region $y=6.75-6.50$ can be identified with the ortho II structure of ideal oxygen stoichiometry $y=6.5$, characterized with regular alternation of Cu-O chains and Cu rows in CuO_δ plane. The observed orthorhombicity $b-a=0.015$ Å is again smaller than that of 0.042–0.044 Å observed on single crystal[9] and powder samples[4] of the $YBa_2Cu_3O_{6.5}$ stoichiometry. The reason why the ortho II type is not realized for the $Y_{0.8}Ca_{0.2}Ba_2Cu_3O_y$ samples with $y\leqslant6.50$ may be related namely to the lower orthorhombicity and, consequently, to a competition of another superstructure of ideal $y=6.5$ stoichiometry (the ''herringbone'' structure[9]) which forms the Cu-O-Cu dimers instead of infinite chains. We anticipate that namely these dimers exist in the third (tetragonal) superconducting phase for $y=6.50-6.40$ and persist possibly even in the nonsuperconducting region $y=6.40-6.03$.

The interatomic distances displayed for the $Y_{0.8}Ca_{0.2}Ba_2Cu_3O_y$ samples in Table II (maximum standard deviation of about 0.01 Å) show some significant changes of cation-oxygen lengths with decreasing *y*. The most marked feature is the increase of the distance between copper in the CuO_2 planes (Cu2 site) and the apical oxygen O1. Barium ions move steadily out of both the O1 and the gradually depleting O4 sites and approach the O2 and O3 sites in the CuO_2 planes. Similar shifts were reported previously for the calcium free system. A significant difference concerns the

TABLE II. Neutron diffraction data obtained for $Y_{0.8}Ca_{0.2}Ba_2Cu_3O_y$.

Composition	y	6.89(3)	6.52(2)	6.50(2)	6.33(2)	6.13(2)
Lattice parameters	a	3.8341	3.8502	3.8586	3.8580	3.8585
	b	3.8735	3.8650	3.8586	3.8580	3.8585
	c	11.668	11.719	11.729	11.754	11.776
Atom coordinates						
Cu1 [0 0 0]						
Cu2 [0 0 z]	z	0.3564(6)	0.3596(5)	0.3596(5)	0.3606(5)	0.3624(5)
Ba [0.5 0.5 z]	z	0.1867(9)	0.1897(7)	0.1902(7)	0.1919(7)	0.1942(6)
Y, Ca [0.5 0.5 0.5]						
O1 [0 0 z]	z	0.1561(10)	0.1543(7)	0.1554(8)	0.1549(8)	0.1525(8)
O2 [0.5 0 z]	z	0.3747(12)	0.3735(13)	0.3773(4)	0.3773(4)	0.3771(4)
O3 [0 0.5 z]	z	0.3806(13)	0.3792(14)	0.3773	0.3773	0.3771
O4 [0 0.5 0]						
Bond length (Å)						
Cu1-O1	$2x$	1.822	1.808	1.823	1.820	1.797
-O4	$2(y-6)x$	1.936	1.932	1.929	1.929	1.929
Cu2-O2	$2x$	1.929	1.932	1.940	1.939	1.937
-O3	$2x$	1.957	1.946	1.940	1.939	1.937
-O1	$(y-6)x$	2.337	2.406	2.396	2.418	2.472
Ba-O1	$4x$	2.748	2.759	2.758	2.763	2.772
-O2	$2x$	2.926	2.894	2.923	2.911	2.892
-O3	$2x$	2.966	2.939	2.923	2.911	2.892
-O4	$2(y-6)x$	2.902	2.941	2.949	2.967	2.993
Y, Ca-O2	$4x$	2.426	2.436	2.407	2.408	2.412
-O3	$4x$	2.370	2.389	2.407	2.408	2.412

z-level position of Cu2 site with respect to the oxygen O2, O3 plane. In $YBa_2Cu_3O_y$ the out-of-plane displacement of copper decreases only slightly from 0.27 to 0.22 Å.[4] A more pronounced change from 0.25 Å for $y=6.89$ to 0.17 Å for $y=6.13$ is obtained in the present system. This may correlate with the charge transfer to the Cu2 sites due to calcium substitution, which is discussed below.

For a global characterization or parametrization of the actual cation coordination it is useful to calculate the bond valence sums (BVS).[13] The results of this summation, appropriately weighted to allow for observed occupancies of oxygen sites, are given in Fig. 6 and are complemented with calculated BVS for calcium free $YBa_2Cu_3O_y$ using the data of Ref. 4. As pointed out by Brown,[14] the BVS do not always represent the true oxidation state since the interatomic distances are imposed to internal strain. In particular, the Ba-O bonds are in average compressed for $y=7$ and they are stretched for $y=6$. An opposite strain influences the Cu-O bonds. The strains are apparently released at $y=6.65$ for $YBa_2Cu_3O_y$. For other y values a correction must be applied. The strain correction for the Cu1 and Cu2 sites of variable valence consists essentially in a renormalization of calculated BVS with respect to the formal mean copper valence, based on standard oxidation states of Ba, Y, Ca, and O (see Ref. 14 for details).

Similar analysis in the $Y_{0.8}Ca_{0.2}Ba_2Cu_3O_y$ system shows that the internal strains are released for $y=6.55$. If the BVS in $Y_{0.8}Ca_{0.2}Ba_2Cu_3O_y$ are corrected for strain one obtains a very smooth change of the Cu2 oxidation state from 2.27 for $y=6.89$ to 2.05 for $y=6.13$, with an extrapolation to about

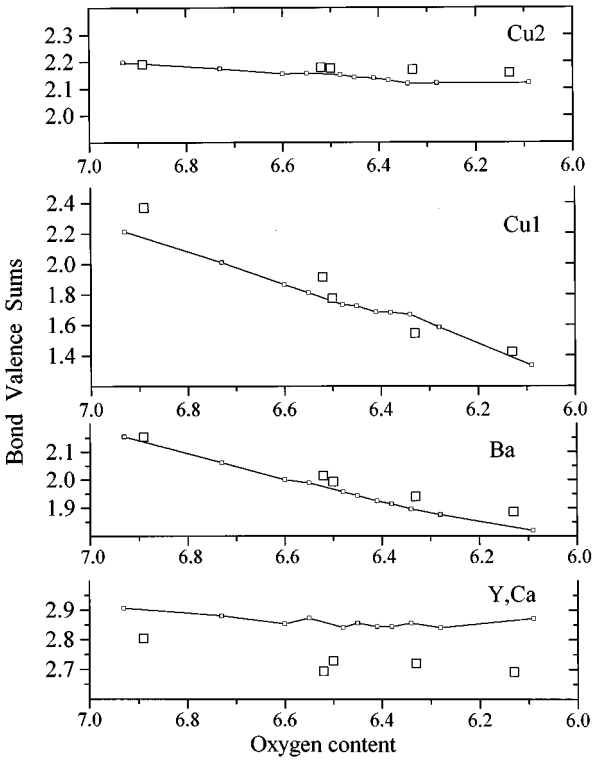

FIG. 6. The calculated BVS for (Y,Ca), Ba, Cu1, and Cu2 sites (large squares) compared with results for the $YBa_2Cu_3O_y$ system of Jorgensen *et al.* (Ref. 4) (lines).

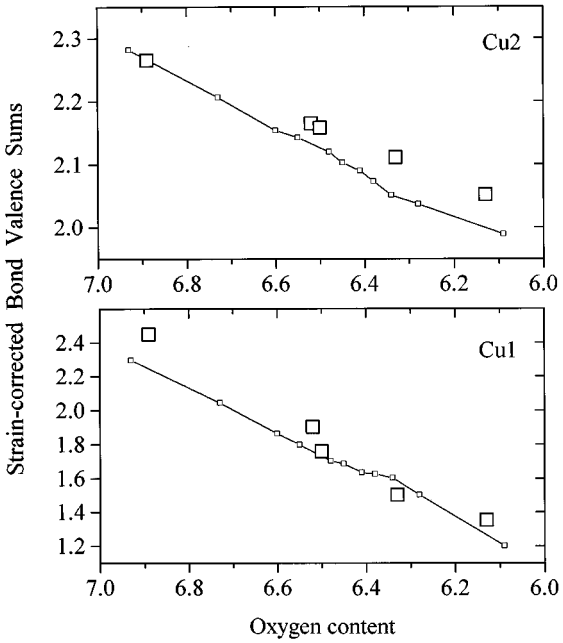

FIG. 7. The bond valence sums of Cu1 and Cu2 after a strain correction following Brown (Ref. 14) (large squares: $Y_{0.8}Ca_{0.2}Ba_2Cu_3O_y$; lines: $YBa_2Cu_3O_y$).

2.00 for $y=6.0$ (see Fig. 7). This essentially linear dependence with the y content means a constant doping into the CuO_2 planes of about 0.6 holes per one added oxygen. The strain corrected Cu1 valence varies in the region $y=6.89-6.13$ from 2.45 to 1.36.

The comparison with the $YBa_2Cu_3O_y$ data in Fig. 7 suggests that for the oxygen rich sample $y=6.89$ the calcium substitution generates additional holes in the Cu-O chains only, whereas for the oxygen deficient sample $y=6.13$ majority of additional holes enter the CuO_2 planes. Nevertheless, this charge transfer due to calcium substitution is not sufficient to preserve superconductivity down to low oxygen stoichiometry.

The corrected bond valence sums of the Cu1 atom in $Y_{0.8}Ca_{0.2}Ba_2Cu_3O_y$ display a marked drop near the orthorhombic-tetragonal transition at $y=6.5$. This anomaly does not occur in the calcium free system $YBa_2Cu_3O_y$—see Fig. 7. We assume that this irregularity does not mean any departure from linear dependence of the true oxidation state of Cu1. Instead, it may indicate that the arrangement of the CuO_δ plane has changed suddenly and the bonds occurred in a tensile strain imposed by the most rigid part of the structure, the CuO_2 plane. This suggests that the tetragonal phase corresponds to the ''herringbone'' structure of Cu-O-Cu dimers rather than to a disorder of Cu-O chain segments. We should add that in that case the true in-plane bond lengths become uncertain and the calculated Cu1 sums in the tetragonal region are in some doubt.

In contrary to the bond strength summation which characterizes the hole distribution between the CuO_2 and CuO_δ planes but does not specify their character, the electric transport properties carry an information on the itinerant carriers. An important information can be inferred from the thermopower data. The absolute values and temperature dependencies, shown in Fig. 1, are in general agreement with findings on high-temperature superconductors which possess the conducting CuO_2 planes only and for which a universal correlation between thermopower data and superconducting properties has been reported.[15] The onset of superconductivity correlates well with a critical value $S_{290}\sim 60\ \mu V\ K^{-1}$ and a maximum T_c is achieved for the sample with $S_{290}\sim 0\ \mu V\ K^{-1}$. In that case the $S(T)$ dependence is linear below 300 K and sharply drops to zero at T_c. This behavior seems to make questionable any significant contribution of Cu-O chains to the electrical conduction in the present $Y_{0.8}Ca_{0.2}Ba_2Cu_3O_y$ samples. With respect to the influential role of the oxygen ordering in the CuO_δ planes on superconductivity, the Cu-O chains should affect the carrier transport rather indirectly via the charge transfer from the CuO_δ to CuO_2 planes.

The normal state resistivity in metallic $Y_{0.8}Ca_{0.2}Ba_2Cu_3O_y$ samples gradually increases with decreasing oxygen content. This increase is accompanied with a decrease of itinerant carrier concentration, manifested by an increase of the Hall constant R_H. As a result, the carrier mobility remains practically constant. The data summarized in Table III show further that the superconductivity and the metallic character of the normal state resistivity vanishes if the carrier concentration is lowered under certain critical value ($n\sim 0.08$ hole/Cu2). The nonsuperconducting region is further characterized by a the sudden decrease of the Hall number and the temperature activation of the Hall constant. All above mentioned indications together with the discrepancy between the hole concentration deduced either from the Hall effect or from the bond strength summation indicate a localization of carriers in the nonsuperconducting samples below 300 K. Despite this qualitative change, the value of Hall mobility at 200 K is comparable to metallic samples—see Table III.

TABLE III. The Hall mobility μ_H and number of itinerant carriers n_H per copper atom in the CuO_2 plane deduced from the resistivity and Hall effect data at 200 K. The formal hole concentration n_{BVS} follows from the bond strength summation for the Cu2 site.

y	ρ ($10^{-5}\ \Omega$ m)	R_H (10^{-9} m^3 C^{-1})	μ_H (10^{-4} m^2/V s)	n_H (hole/Cu2)	n_{BVS} (hole/Cu2)
6.89	1.2	2	1.7	0.27	0.27
6.52	2.5	4	1.6	0.14	0.17
6.50	5	7	1.4	0.08	0.16
6.36	8	7	0.9	0.08	0.12[a]
6.33	30	60	2.0	0.01	0.11

[a]Interpolated value.

V. CONCLUSION

The $Y_{0.8}Ca_{0.2}Ba_2Cu_3O_y$ samples with a large range of oxygen content $y=6.89-6.03$ have been prepared under reducing or oxidizing conditions and were equilibrated at 460 °C. Their complex study has shown that the superconductivity occurs for $y \geq 6.4$. Earlier reported superconductivity for $y=6.0-6.2$ should be likely ascribed to a surface oxidation of crystal grains in quenched samples.

The investigation of the structure, electric transport, and diamagnetism in $Y_{0.8}Ca_{0.2}Ba_2Cu_3O_y$ evidenced the important role of the oxygen ordering in the CuO_δ planes for the superconductivity. Contrary to the two superconducting plateaus found for $YBa_2Cu_3O_y$ with $T_c=90$ and 60 K, three-plateau behavior was observed and was identified with crystallographically different phases in the present system. The first two plateaux correspond to phases with T_c of 80 K ($6.89 \geq y \geq 6.75$) and 50 K ($6.75 \geq y \geq 6.50$) and are associated with the ortho I and II structures, characterized with infinite Cu-O chains. The third plateau corresponds to macroscopically tetragonal phase with $T_c=25$ K ($6.50 \geq y \geq 6.40$) and is possibly associated with formation of the Cu-O-Cu dimers. Moreover, each phase exhibits a distinct value of the room-temperature thermopower coefficient which is preserved over the respective regions.

All three superconducting phases in $Y_{0.8}Ca_{0.2}Ba_2Cu_3O_y$ exhibit sharp magnetic transitions with nearly complete diamagnetism at low temperatures and a metalliclike electric conductivity in the normal state. The situation is dramatically changed at the transition to the nonsuperconducting region below $y=6.4$ where a sudden localization of carriers is observed.

ACKNOWLEDGMENTS

The research was performed under a support of the Grant Agency of ASCR (Grant No. A110408). One part of the work was carried out under the financial support of the Belgian Office for Scientific, Technical, and Cultural Affairs in Louvain-la-Neuve, Unité de Physico-Chemie et de Physique des Matériaux, UCL, Belgium. One of the authors (J.H.) would like to acknowledge this support and to thank J. P. Issi, E. Grivei, and S. Dubois for helpful discussions. We are grateful to D. Zemanová for the chemical analyses.

[1] A Manthiram, S. J. Lee, and J. B. Goodenough, J. Solid State Chem. **73**, 278 (1988).

[2] Z. Jirák, J. Hejtmánek, E. Pollert, A. Tříska, and P. Vašek, Physica C **156**, 750 (1988).

[3] E. M. McCarron, M. K. Crawford, and J. B. Parise, J. Solid State Chem. **78**, 192 (1989); J. B. Parise and E. M. McCarron, *ibid.* **83**, 188 (1989); R. S. Liu, J. R. Cooper, J. W. Loram, W. Zhou, W. Lo, P. P. Edwards, and W. Y. Liang, Solid State Commun. **76**, 679 (1990); C. Legros-Gledel, J.-F. Marucco, E. Vincent, D. Favrot, B. Poumellec, B. Touzelin, M. Gupta, and H. Alloul, Physica C **175**, 279 (1991); H. Casalta, H. Alloul, and J.-F. Marucco, *ibid.* **204**, 331 (1993).

[4] J. D. Jorgensen, B. W. Veal, A. P. Paulikas, L. J. Nowicki, G. W. Crabtree, H. Claus, and W. K. Kwok, Phys. Rev. B **41**, 1863 (1990).

[5] R. J. Cava, A. W. Hewat, E. A. Hewat, B. Batlogg, M. Marezio, K. M. Rabe, J. J. Krajewski, W. F. Peck, Jr., and L. W. Rupp, Jr., Physica C **165**, 419 (1990).

[6] J. A. Osborn, Phys. Rev. **67**, 351 (1945).

[7] D. Hohlwein, in *Materials and Crystallographic Aspects of HT_c-Superconductivity*, Vol. 263 of *NATO Advanced Study Institute, Series E*, edited by E. Kaldis (Kluwer Academic, Dordrecht, The Netherlands, 1994), p. 65.

[8] R. Sonntag, D. Hohlwein, T. Bruckel, and G. Collin, Phys. Rev. Lett. **66**, 1497 (1991).

[9] Th. Zeiske, D. Hohlwein, R. Sonntag, F. Kubanek, and G. Collin, Z. Phys. B **86**, 11 (1992).

[10] J. Grybos, D. Hohlwein, Th. Zeiske, R. Sonntag, F. Kubanek, K. Eichhorn, and Th. Wolf, Physica C **220**, 138 (1994).

[11] P. Schleger, R. A. Hadfield, H. Casalta, N. H. Andersen, H. F. Poulsen, M. von Zimmermann, J. R. Schneider, Ruixing Liang, P. Dasanjh, and W. N. Hardy, Phys. Rev. Lett. **74**, 1446 (1995).

[12] A. Stratilatov, V. Plakhty, Yu. Chernenkov, and V. Fedorov, Phys. Lett. A **180**, 137 (1993); K. Ruck, H. Borrmann, and A. Simon, Solid State Commun. **93**, 865 (1995).

[13] I. D. Brown, Acta Crystallogr. B **41**, 244 (1985).

[14] I. D. Brown, J. Solid State Chem. **90**, 155 (1991).

[15] S. D. Obertelli, J. R. Cooper, and J. L. Tallon, Phys. Rev. B **46**, 14 928 (1992).